Current Biology 24, 868–874, April 14, 2014 ©2014 Elsevier Ltd All rights reserved http://dx.doi.org/10.1016/j.cub.2014.02.057

Report

E-Cadherin-Mediated Cell Coupling Is Required for Apoptotic Cell Extrusion

Veronica Lubkov[1] and Dafna Bar-Sagi[1,*]
[1]Department of Biochemistry and Molecular Pharmacology, New York University School of Medicine, New York, NY 10016, USA

Summary

Apoptotic extrusion is a multicellular process utilized by live cells to remove neighboring apoptotic cells. In epithelial tissues, this process has been shown to be critical for the preservation of tissue integrity and barrier function [1, 2]. Here we demonstrate that extrusion is driven by the retraction of the apoptotic cell, which, in turn, triggers a transient and coordinated elongation of the neighboring cells. The coordination of cell elongation requires E-cadherin-mediated cell-cell adhesion. Accordingly, cells that express low levels of E-cadherin are compromised in elongation and apoptotic extrusion, and furthermore, display loss of barrier function in response to apoptotic stimuli. These findings indicate that the maintenance of adhesive forces during apoptotic cell turnover might play an essential role in controlling tissue homeostasis.

Results and Discussion

Apoptosis is the most common mechanism by which unwanted cells are eliminated in epithelial tissues [1–7]. The process by which apoptotic cells are removed from the epithelium has been termed extrusion and involves the squeezing out of the dying cell as a consequence of contractile forces exerted by its neighboring live cells [1, 8]. Although some of the regulatory pathways that contribute to apoptotic extrusion have been elucidated, the mechanisms by which this multicellular response is coordinated remain largely unknown.

To address this question, we have employed an experimental system in which the dynamics of the response of epithelial monolayers to apoptotic stimuli can be assessed with high spatial and temporal specificity. A salient feature of this system is the induction of apoptosis at the single-cell level by the nuclear injection of a plasmid driving expression of a truncated form of a proapoptotic member of the Bcl2 family Bid (tBid) [9]. As illustrated in Figure 1A and Figures S1A and S1B (available online), the injection of tBid into a Madin-Darby canine kidney (MDCK) cell induced phenotypic changes that are characteristic of apoptotic cell death, including cell blebbing and shrinkage, the formation of a contractile actin ring, the acquisition of a phase-bright appearance marking the vertical displacement of the cell undergoing extrusion, and the eventual detachment of the dying cell from the monolayer within 30–100 min postextrusion (data not shown). A similar pattern of morphological progression has been previously described for apoptosis induced by the injection of cytochrome *c* [10, 11].

We have applied live-cell imaging to simultaneously follow the dying cell and its live neighbors. Real-time changes in cell morphology were analyzed using software that manually segments cell contours (Figure 1A). In order to morphometrically characterize live cells, we measured $\Delta_t S$, the derivative of the ratio between the major and the minor axis of the cell (S) (Figure 1A, bottom). This dimensionless aspect ratio normalizes the variation in size and shape that is inherent to unperturbed MDCK cells. The dying cell was morphometrically characterized by measurement of the cell area, A' (the total number of pixels within the marked cell boundaries), which reports cell shrinkage, a hallmark of apoptosis [12]. We have found that the living cells in direct contact with the apoptotic cells underwent elongation in the direction of the apoptotic cell (Figure 1B; Movie S1, left; Figure S1C). The elongation was transient, reaching peak values at the time of cell extrusion (Figure 1B) and culminating with cell relaxation (Figure S1D). In contrast, no elongation was detected in cells that are not in direct contact with the apoptotic cell or in mock-injected monolayers (Figures S1E and S1F).

It has been demonstrated that apoptotic extrusion depends on the contraction of the actomyosin network in the cells that surround the apoptotic cell [1]. The contraction is mediated by the small GTPase Rho [1, 13–15]. Accordingly, injection of C3 transferase, a specific Rho inhibitor [16], into the neighboring cells has been shown to abolish actomyosin contraction and block apoptotic extrusion [1]. Several lines of evidence suggest that the observed elongation of the live cells is dependent on Rho-mediated contractility of the actomyosin network. First, as illustrated in Figure S1G, C3-transferase-injected cells failed to elongate in response to tBid-induced apoptosis. Second, we have observed that the dynamics of cell elongation closely follows the dynamics of actin recruitment at the ring that surrounds the apoptotic cell (measured using the actin probe mCherry-Utrophin; see Figures 1C and 1D; Movie S1, middle). Lastly, we have found that cell elongation correlated with the levels of active myosin, a marker of cell contractility (Figure S1H), and with the levels of Vinculin at cell-cell junctions (Figure S1I), which are sites of myosin-dependent tension [17].

We observed that the elongation of the live cells is initiated only after the dying cell has undergone considerable shrinkage (Figure 1B). This temporal relationship between the increase in elongation of live cells and the apoptotic progression of the dying cell raises the possibility that cell elongation might be functionally coupled to the morphological changes in the apoptotic cell. To test this idea, we sought to analyze the response of the epithelial monolayer under conditions where apoptosis-related morphological changes can be uncoupled from cell death. To this end, we microinjected a constitutively active form of the Rho-associated coiled-coil-containing protein ROCK (ΔROCK2) [18]. In agreement with earlier reports [18–20], we have observed that MDCK cells injected with ΔROCK2 acquired morphological changes that are characteristic of apoptotic cell death, most notably cell shrinkage in the absence of an actual cell death as determined by Annexin V-fluorescein isothiocyanate staining (Figure S1J). Importantly, the expression of ΔROCK2 elicited transient elongation of the neighboring cells and cell extrusion similar to that observed upon the induction of apoptosis (Figures 1E, 1F, and S1K; Movie S1, right). These results indicate that the morphological changes that take place as the cell undergoes

*Correspondence: dafna.bar-sagi@nyumc.org

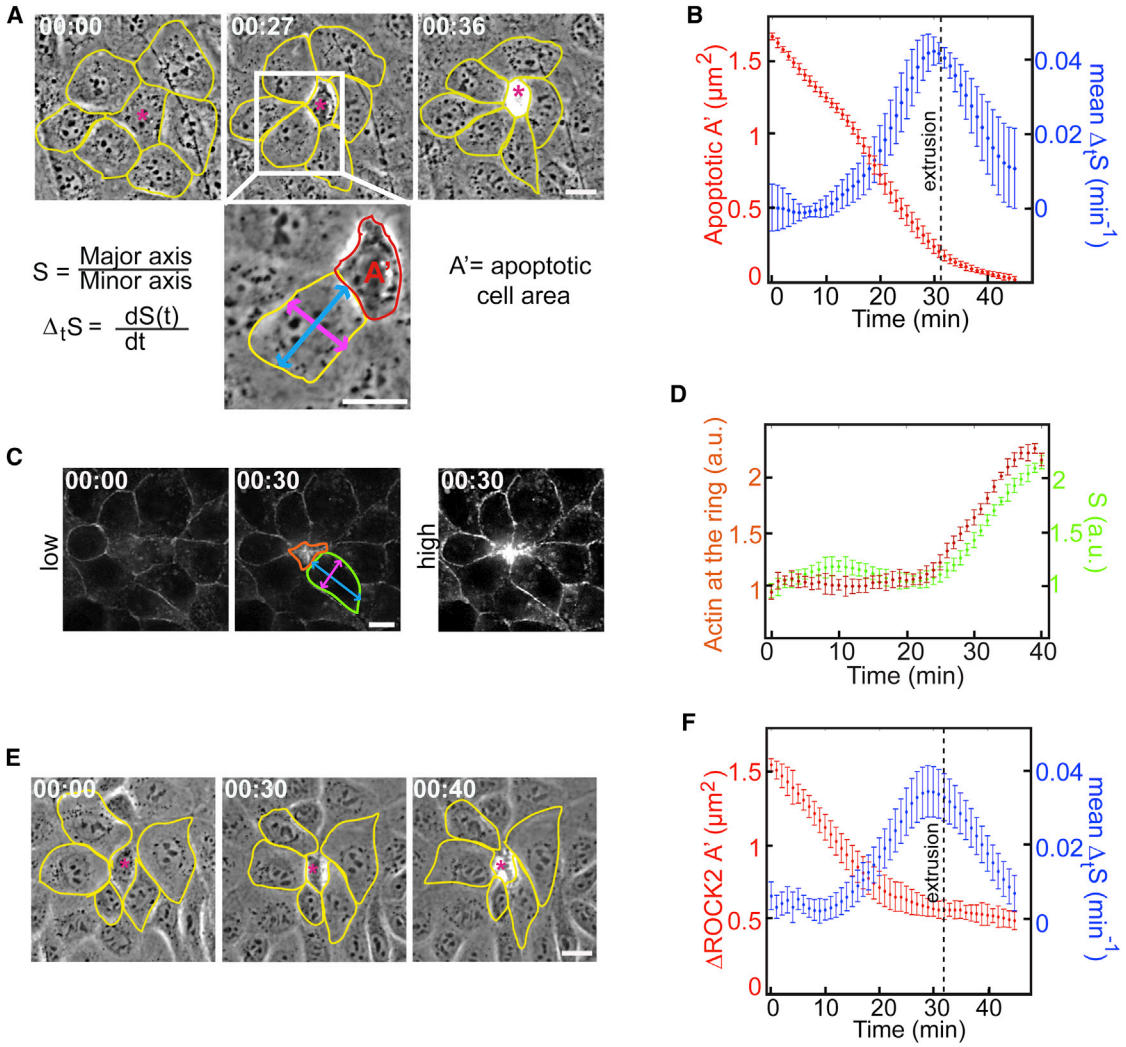

Figure 1. Contractility Based Cell Elongation Is Required for Apoptotic Extrusion

(A) Top: representative images from a phase-contrast time-lapse movie of an MDCK cell undergoing apoptosis (asterisk) after the microinjection of pCMV-tBid plasmid. Manual segmentation (MATLAB) of the neighboring cells is shown in yellow, and t = 0 is defined as the time when morphological changes in the apoptotic cell are first detected. Inset time is shown in hr:min. Scale bar, 10 μm. Bottom: enlargement of the top image indicating the parameters used for quantifying changes in the cell shape of neighboring cells (S) (major axis [blue] and minor axis [magenta] ratio), its temporal derivative ($\Delta_t S$), and apoptotic cell area (A′) (red).

(B) Mean $\Delta_t S$ distribution plot of cells in direct contact with the apoptotic cell (blue) and A′ of the tBid-injected apoptotic cell (red). Error bars represent SEM from n = 5 independent experiments. Dotted line indicates acquisition of phase-bright rounded appearance, which marks the apical displacement of the injected cell.

(C and D) Representative fluorescent images from a time-lapse movie of MDCK cells stably expressing mCherry-Utrophin (C) and plot of the actin intensity (orange) surrounding the apoptotic cell and mean S of the neighboring cells (green) as a function of time (D). Images in (C) labeled as "low" are captured with an exposure time that is sufficient to allow for the quantification as shown in (D), whereas the image labeled "high" is oversaturated for demonstration purposes only. Error bars represent SEM from n = 3 independent experiments. Inset time is shown in hr:min. a.u., arbitrary units.

(E) Representative phase-contrast images from a time-lapse movie of MDCK cells after the microinjection of a ΔROCK2 expression plasmid. The injected cell is marked with an asterisk. Manual segmentation (MATLAB) of the neighboring cells is shown in yellow. Error bars represent SEM from n = 5 independent experiments. Scale bar, 10 μm.

(F) Mean $\Delta_t S$ distribution plot of cells in direct contact with the ΔROCK2-expressing cell (blue) and A′ of the ΔROCK2-expressing cell (red). Error bars represent SEM from n = 4 independent experiments. Dotted line indicates acquisition of phase-bright rounded appearance, which marks the apical displacement of the injected cell.

See also Figure S1 and Movie S1.

apoptotic death may be sufficient to trigger the elongation of the surrounding living cells.

Apoptotic cell death is characterized by the retention of cell membrane integrity [21]. As such, the morphological changes displayed by the living cells could result from the pulling force that the apoptotic cell would exert as it shrinks. To investigate this possibility, we have analyzed the consequences of necrosis, a cell death modality that is associated with a loss of structural integrity of the plasma membrane [21–23]. To induce necrosis, single cells were mechanically punctured using the tip of a microneedle. The resulting loss of membrane integrity was demonstrated by the uptake of the

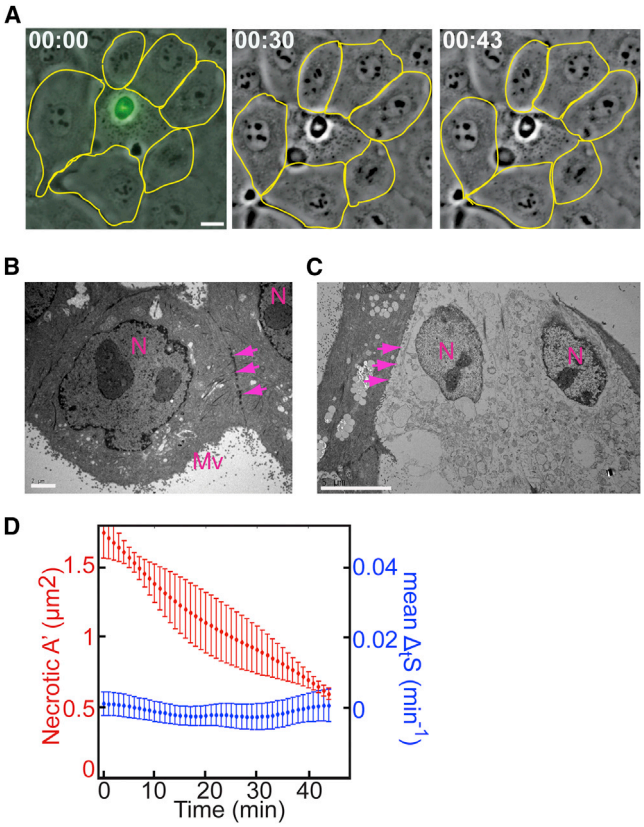

Figure 2. Live Cell Elongation Is Mediated by Contact-Dependent Pulling Forces Exerted by the Dying Cell

(A) Representative images from a time-lapse movie of a MDCK cell undergoing necrosis (marked in the first panel with SYTOX Green). Manual segmentation (MATLAB) of the neighboring cells is shown in yellow. Inset time is shown in hr:min. Scale bar, 10 μm.

(B and C) Transmission electron microscopy micrographs of unperturbed and necrotic MDCK cells. (B) A representative image of unperturbed MDCK cells, indicating microvilli (Mv) protruding from the entire surface, a smoothly outlined nucleus (N), and cell-cell junctions (marked with arrows). (C) Necrotic MDCK cells display dismantled cytoplasm and a loss of plasma membrane integrity (arrows). Scale bars, 2 μm (B) and 5 μm (C).

(D) Mean $\Delta_t S$ distribution plot of cells in direct contact with necrotic cells (blue), and A' of the necrotic cell (red). Error bars represent SEM from n = 5 independent experiments.

See also Figure S2 and Movie S2.

membrane-impermeant dye SYTOX Green (Figure 2A), electron microscopy analysis (Figures 2B and 2C), and analysis of cell-cell contacts as determined by live imaging of MDCK cells stably expressing E-cadherin-GFP [24] (Figures S2A and S2B; Movie S2, left). Importantly, the induction of necrosis failed to initiate elongation in the neighboring cells (Figures 2A and 2D; Movie S2, right). These observations are consistent with the hypothesis that contact-dependent pulling forces from the apoptotic cell trigger the elongation of its neighboring cells.

To further investigate the dynamics of cell shape changes in response to apoptosis, we have analyzed the temporal relationships between the elongation of neighboring cells. A heatmap display of $\Delta_t S$ values for nearest neighbors indicates that the majority of cells elongated in a highly coordinated manner (Figures 3A and S3A). To test the physiological relevance of this coordination, we blocked elongation of a subset of cells that are in direct contact with the dying cell by microinjecting with C3 transferase (Figure 3B). Elongation was reduced by ~2-fold in noninjected cells (Figure 3C versus Figure 1B). Moreover, when three to five neighboring cells were injected with C3 transferase (out of typically six to seven cells), the remaining noninjected cells failed to extrude the apoptotic cells (Figure S3B; Movie S3, left) as evident by in-plane position of the apoptotic cell. This observation supports a role for a coordinated response by the neighboring cells in the apoptotic extrusion process.

Cell-cell adhesion plays an important role in coordinating cell behavior [25–27]. To investigate the contribution of intercellular junctions to the elongation response and apoptotic cell extrusion, we examined the effects of depletion of E-cadherin, a critical modulator of cell-cell contact. This was accomplished through the generation of stable MDCK cell lines expressing doxycycline-inducible small hairpin RNA (shRNA) constructs targeting different regions of canine E-cadherin (shEcad A and B) as well as shRNA (scramble) control. The efficiency of knockdown was confirmed by immunofluorescence, immunoblotting, and RT-PCR (Figures 3D, 3E and S3C). We found that MDCK cells depleted of E-cadherin failed to elongate and extrude the dying cell (Figure 3F; Movie S3, middle and right), as assessed by the in-plane position of the apoptotic cell for the duration of the experiment. The failure to elongate was not merely due to an inability of the neighboring cells to assemble an actin ring, because the formation of the ring around the apoptotic cell was unperturbed in the E-cadherin-depleted MDCK monolayer (Figures S3D and S3E). These findings indicate that E-cadherin-mediated adhesion is required for both cell elongation and apoptotic extrusion. The extent to which elongation is causally linked to extrusion remains to be established.

Loss of E-cadherin expression has been often associated with epithelial cancers [28]. In light of our observation that E-cadherin-mediated adhesion is required for cell elongation, we set out to test the prediction that the capacity of cancer cell lines to elongate in response to apoptosis is dependent on their E-cadherin status. In human cancer cell lines that are E-cadherin positive, such as 5637, H441, and Caco-2 (Figures 4A and 4B; Movie S4, left), the induction of apoptosis was accompanied by transient elongations in the neighboring cells with similar dynamics to those observed in MDCK cells (Figure 1B). In contrast, E-cadherin-deficient cell lines, such as T24, A549, PANC-1, and SW480, failed to elongate (Figures 4A, 4C, and 4E; Movie S4, right). To confirm that the inability to elongate is due specifically to loss of E-cadherin, we analyzed whether restoring E-cadherin could rescue the ability of the cells surrounding the apoptotic cells to elongate. Stable expression of E-cadherin fused directly to α-catenin (E-cad-α-cat) [29] (a mutant that lacks the β-catenin binding region and therefore regulates E-cadherin-mediated adhesion, but not gene expression) restored both intercellular adhesion (Figure 4D) and the ability of neighboring cells to undergo the morphological changes required for apoptotic extrusion (Figure 4E).

It has been proposed that the contraction of the neighboring cells around the dying cell serves to prevent the formation of a gap in the epithelial monolayer that could result from the exit of the apoptotic cell [1, 2, 30]. This raises the possibility that impaired elongation could result in a breach in the epithelial barrier function. In support of this prediction, we have found that E-cadherin-depleted MDCK cells often formed gaps in the monolayer around the dying cell (Figures 4F, S3D, and S3F; Movie S3, middle). To test whether this disruption in the

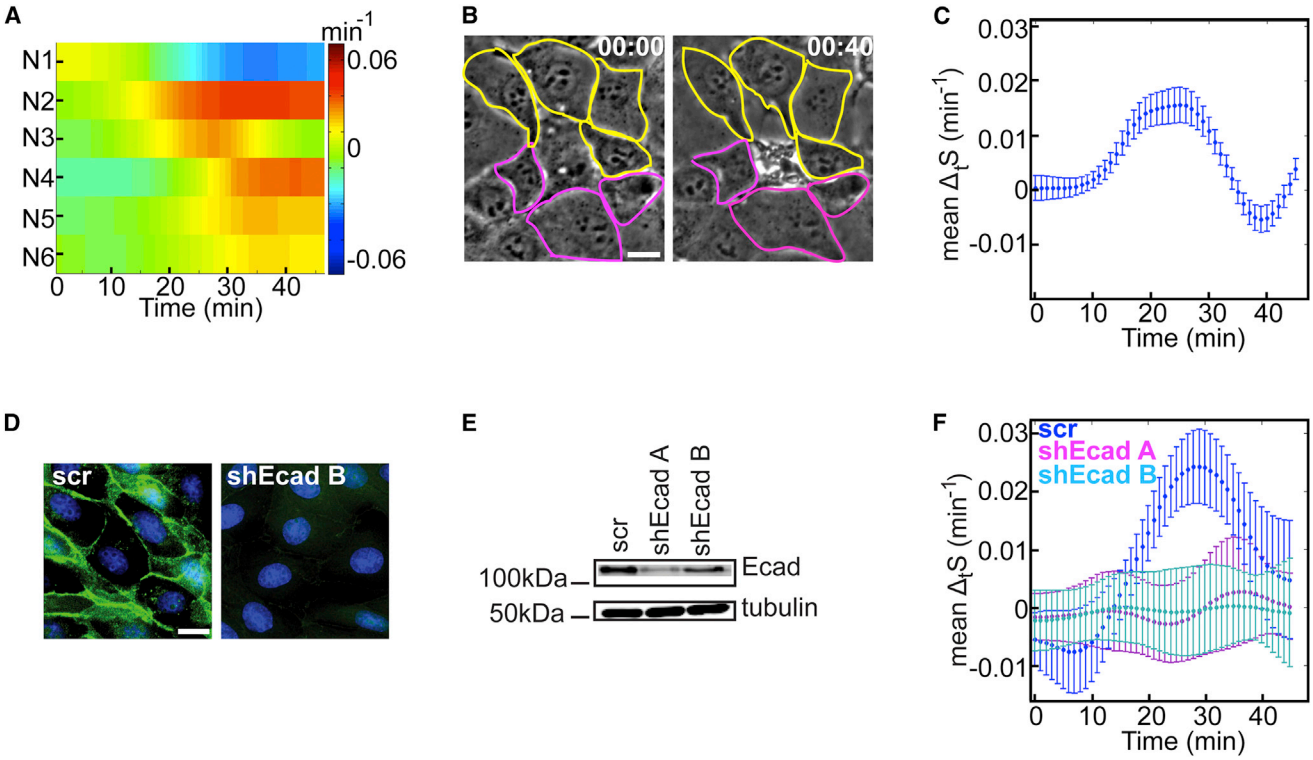

Figure 3. E-Cadherin-Dependent Coordinated Elongation of Neighboring Cells Is Required for Apoptotic Extrusion

(A) Elongation rates of individual cells in contact with the apoptotic cell depicted as a heat map in which $\Delta_t S$ is displayed as a function of time. Each row represents $\Delta_t S$ for an individual neighboring cell (N1–N6). Data are representative of 10 independent experiments.

(B) Time-lapse images of a MDCK cell undergoing apoptosis (center). The C3-transferase-microinjected cells and noninjected neighboring cells are outlined in pink and yellow, respectively. Image is a representative of n = 8 independent experiments. Inset time is shown in hr:min. Scale bar, 10 μm.

(C) The mean $\Delta_t S$ distribution plot demonstrating the effect of C3 transferase on noninjected cells in direct contact with the apoptotic cell. Error bars represent SEM from n = 5 independent experiments.

(D–F) MDCK cells stably expressing inducible shRNA targeting E-cadherin (shEcad A or B) or scrambled shRNA (scr), as indicated, were induced with doxycycline for 6 days. (D) Immunofluorescence analysis of E-cadherin distribution (green) in MDCK cells expressing the indicated shRNAs. DAPI (blue) stains nuclei. Scale bar, 10 μm. (E) Cell lysates were immunoblotted with an anti-E-cadherin antibody. Anti-β-tubulin was used as a loading control. (F) Mean $\Delta_t S$ plots of MDCK cells depleted of E-cadherin, shEcad A and B (magenta and turquoise), compared with control cells, expressing scramble hairpin (blue) after the induction of apoptosis. Error bars represent SEM from n = 3 independent experiments.

See also Figure S3 and Movie S3.

continuity of the monolayer was associated with the loss of epithelial barrier function, we carried out permeability measurements on polarized MDCK monolayers [31]. To this end, MDCK cells were plated on Transwell filters and allowed to grow to confluence in the presence of doxycycline to induce knockdown of E-cadherin. Junction integrity after UV-induced apoptosis was then assessed by uptake of paracellular fluorescent dextran. As illustrated in Figure 4G, the induction of apoptosis in epithelial monolayers that lack E-cadherin was associated with an increased paracellular diffusion of fluorescent dextran consistent with a disruption in barrier function. The specificity of this effect is indicated by the observations that E-cadherin depletion had no effect on the extent of apoptotic cell death (Figures S4A and S4B) or the epithelial barrier function itself in the absence of apoptotic stimuli, as assessed by localization of tight-junction-associated zona occludens-1 [32] (Figure S4C). It has been shown that loss of barrier function could result from cell separation induced by high levels of cell contractility [33]. To examine the relevance of this mechanism to the breach in barrier function observed in the E-cadherin-depleted cells, we abrogated actomyosin contractility by using the ROCK inhibitor Y-27632. As shown in Figure S4D, the enhanced permeability displayed by E-cadherin-depleted cells after apoptosis was significantly reduced by ROCK inhibition, suggesting a role for E-cadherin in coordinating the transmission of contractile forces between neighboring cells. Together, these results indicate that E-cadherin status may be an important determinant in preserving the barrier function of epithelial cells when exposed to apoptotic stimuli.

Mechanical signals have been implicated in the regulation of multiple fundamental biological processes, such as cell growth, differentiation, and tissue development and maintenance [7, 34, 35]. Our findings that ROCK-dependent morphological changes are necessary and sufficient to trigger cell extrusion suggest that mechanical signals from the apoptotic cell might play an essential role in regulating this process. It has been previously proposed that the release of a soluble factor, sphingosine 1-phosphate, by the dying cell promotes the contraction of the neighboring cells, thereby triggering cellular extrusion [36]. Future studies will be required to dissect how these different mechanisms might mutually contribute to the dynamics and robustness of apoptotic cell extrusion.

A key feature of the coordinated response of the neighboring cells to the dying cell, as revealed in the present study, is its

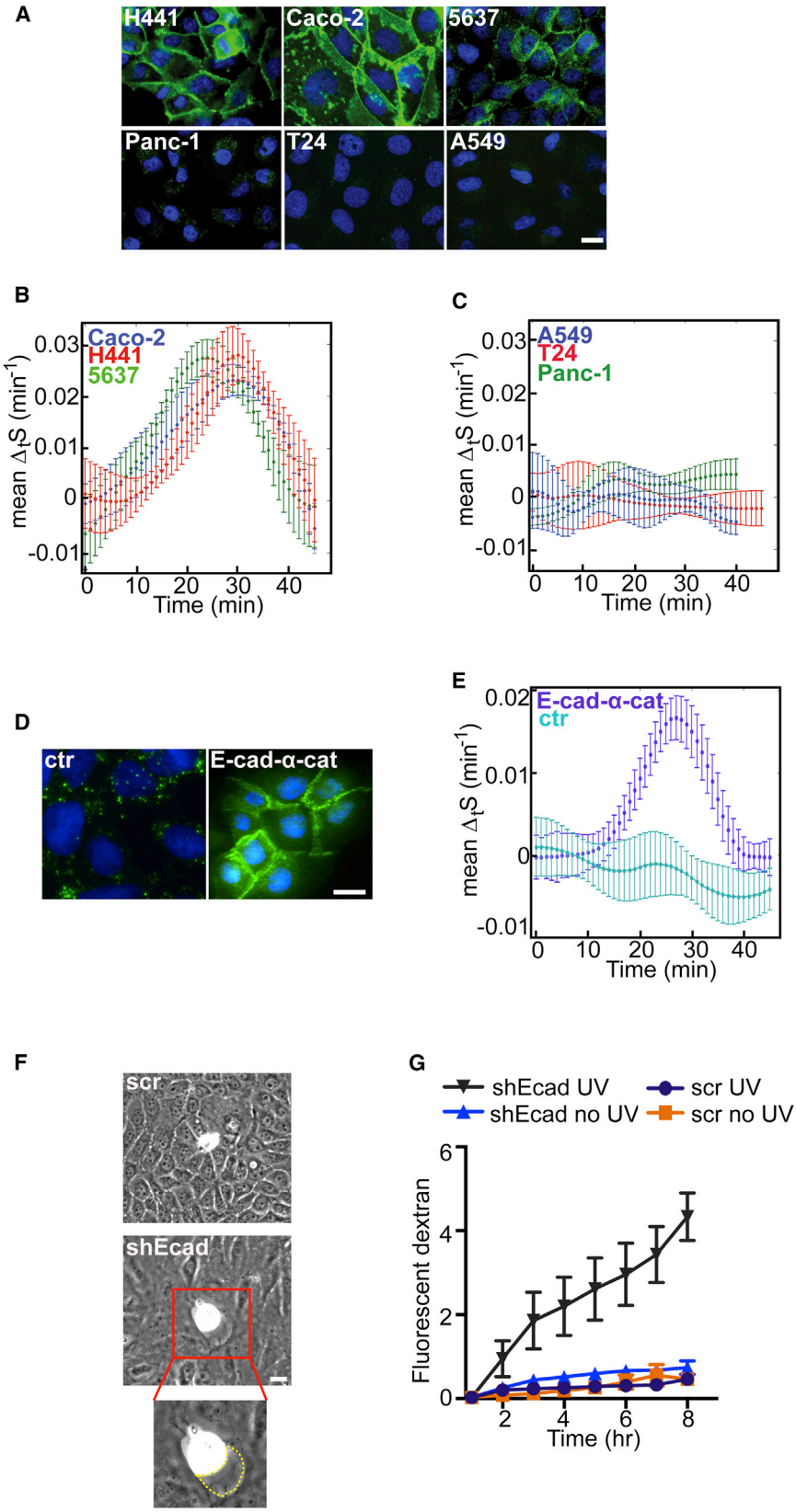

Figure 4. Cell-Cell Adhesion Is Required for Maintaining Epithelial Integrity and Barrier Function during Apoptotic Extrusion

(A) Indirect immunofluorescence was used to detect E-cadherin distribution (green) in the human cancer cell lines indicated. DAPI (blue) stains nuclei. Scale bar, 20 μm.

(B and C) Mean $\Delta_t S$ plots of E-cadherin-positive (B) and E-cadherin-negative (C) human cancer cells after the induction of apoptosis. Error bars represent SEM from n = 3 independent experiments for each cell line.

(D) Indirect immunofluorescence was used to detect E-cadherin distribution (green) in SW480 control cells (ctr) and SW480 cells stably expressing E-cad-α-cat. An antibody against the extracellular domain of E-cadherin (HECD-1) was used. DAPI (blue) stains nuclei. Scale bar, 20 μm.

(E) Mean $\Delta_t S$ distribution of SW480 control cells (turquoise) and SW480 cells expressing E-cad-α-cat (purple). Error bars represent SEM from n = 3 independent experiments.

(F) Images from phase-contrast time-lapse movies at the time points indicated showing MDCK control cells (scr) and E-cadherin-depleted MDCK cells (shEcad) undergoing apoptosis. The enlargement of the outlined area indicates gaps (dotted line) formed around the E-cadherin-depleted dying cell. Scale bar, 20 μm.

(G) Paracellular tracer permeability assay in E-cadherin-depleted MDCK cells (shEcad) or control cells (scr). Measurements were taken every hour after treatment with UV or under basal conditions, as indicated. Error bars represent SEM from n = 3 independent experiments.

See also Figure S4 and Movie S4.

dependence on E-cadherin. The requirement for E-cadherin likely reflects multiple regulatory roles, including the maintenance of adhesion forces between the live cells as well as between the apoptotic cell and the surrounding live cell. In addition, E-cadherin could be required to transmit tension around the contractile ring. In *Drosophila* embryos, reducing cell adhesion through injection of E-cadherin-targeted double-stranded RNA leads to failure to maintain tension between cells, causing tissue-wide epithelial tears [37]. By analogy, our data suggest that reduced E-cadherin levels could lead to an impairment of epithelial integrity during cellular turnover.

A breach in epithelial integrity is linked to loss of barrier function and as such could stir leakage of immunostimulatory contents, leading to immune stimulation and secretion of cytokines that can feed back and further increase epithelial leakiness [38, 39]. Because downregulation of E-cadherin-mediated adhesion has been shown to be an early event in tumorigenesis [40–42], apoptotic cell death in this setting could contribute to the establishment of inflammatory conditions. Thus, the link between E-cadherin status and apoptotic cell extrusion may constitute an important determinant of tissue homeostasis under normal physiology as well as under pathological conditions.

Experimental Procedures

Standard procedures were followed as described in the Supplemental Experimental Procedures. All error bars indicate SEM, unless noted. The p values have been derived by two-tailed t test or chi-square test as indicated. Image segmentation was performed manually using custom designed MATLAB software (MathWorks).

Supplemental Information

Supplemental Information includes Supplemental Experimental Procedures, four figures, and four movies and can be found with this article online at http://dx.doi.org/10.1016/j.cub.2014.02.057.

Acknowledgments

We are grateful to Stefano Di Talia (Princeton University) for developing computational methods for cell-shape analysis and for advice throughout various stages of this project. We thank Jacqueline Bréard (Université Paris-Sud 11), James Nelson (Stanford University), Cara Gottardi (Northwestern University), William Bement (University of Wisconsin-Madison), Tony Huang (New York University School of Medicine), and Ramanuj Dasgupta (New York University School of Medicine) for generously providing reagents. We thank Alice Liang and Yan Deng at the NYU Microscopy Core for transmission electron microscopy analysis and help with the live-cell imaging system, respectively. We also thank Laura Taylor and Elda Grabocka for technical support and all members of the lab for discussions and comments on the manuscript. The rr1 antibody against canine E-cadherin was developed by Gumbiner B. and made available by the Developmental Studies Hybridoma Bank under the auspices of the NICHD.

Received: July 25, 2013
Revised: January 13, 2014
Accepted: February 26, 2014
Published: April 3, 2014

References

1. Rosenblatt, J., Raff, M.C., and Cramer, L.P. (2001). An epithelial cell destined for apoptosis signals its neighbors to extrude it by an actin- and myosin-dependent mechanism. Curr. Biol. *11*, 1847–1857.
2. Madara, J.L. (1990). Maintenance of the macromolecular barrier at cell extrusion sites in intestinal epithelium: physiological rearrangement of tight junctions. J. Membr. Biol. *116*, 177–184.
3. Eisenhoffer, G.T., Loftus, P.D., Yoshigi, M., Otsuna, H., Chien, C.B., Morcos, P.A., and Rosenblatt, J. (2012). Crowding induces live cell extrusion to maintain homeostatic cell numbers in epithelia. Nature *484*, 546–549.
4. Harding, R.K., and Morris, G.P. (1977). Cell loss from normal and stressed gastric mucosae of the rat. An ultrastructural analysis. Gastroenterology *72*, 857–863.
5. Baron, D.A., and Miller, D.H. (1990). Extrusion of colonic epithelial cells in vitro. J. Electron Microsc. Tech. *16*, 15–24.
6. Abrams, J.M., White, K., Fessler, L.I., and Steller, H. (1993). Programmed cell death during Drosophila embryogenesis. Development *117*, 29–43.
7. Toyama, Y., Peralta, X.G., Wells, A.R., Kiehart, D.P., and Edwards, G.S. (2008). Apoptotic force and tissue dynamics during Drosophila embryogenesis. Science *321*, 1683–1686.
8. Bement, W.M. (2002). Actomyosin rings: the riddle of the sphincter. Curr. Biol. *12*, R12–R14.
9. Li, H., Zhu, H., Xu, C.J., and Yuan, J. (1998). Cleavage of BID by caspase 8 mediates the mitochondrial damage in the Fas pathway of apoptosis. Cell *94*, 491–501.
10. Li, F., Srinivasan, A., Wang, Y., Armstrong, R.C., Tomaselli, K.J., and Fritz, L.C. (1997). Cell-specific induction of apoptosis by microinjection of cytochrome c. Bcl-xL has activity independent of cytochrome c release. J. Biol. Chem. *272*, 30299–30305.
11. Brustugun, O.T., Fladmark, K.E., Doskeland, S.O., Orrenius, S., and Zhivotovsky, B. (1998). Apoptosis induced by microinjection of cytochrome c is caspase-dependent and is inhibited by Bcl-2. Cell Death Differ. *5*, 660–668.
12. Mills, J.C., Stone, N.L., Erhardt, J., and Pittman, R.N. (1998). Apoptotic membrane blebbing is regulated by myosin light chain phosphorylation. J. Cell Biol. *140*, 627–636.
13. Bement, W.M., Forscher, P., and Mooseker, M.S. (1993). A novel cytoskeletal structure involved in purse string wound closure and cell polarity maintenance. J. Cell Biol. *121*, 565–578.
14. Chrzanowska-Wodnicka, M., and Burridge, K. (1996). Rho-stimulated contractility drives the formation of stress fibers and focal adhesions. J. Cell Biol. *133*, 1403–1415.
15. Amano, M., Ito, M., Kimura, K., Fukata, Y., Chihara, K., Nakano, T., Matsuura, Y., and Kaibuchi, K. (1996). Phosphorylation and activation of myosin by Rho-associated kinase (Rho-kinase). J. Biol. Chem. *271*, 20246–20249.
16. Chardin, P., Boquet, P., Madaule, P., Popoff, M.R., Rubin, E.J., and Gill, D.M. (1989). The mammalian G protein rhoC is ADP-ribosylated by Clostridium botulinum exoenzyme C3 and affects actin microfilaments in Vero cells. EMBO J. *8*, 1087–1092.
17. le Duc, Q., Shi, Q., Blonk, I., Sonnenberg, A., Wang, N., Leckband, D., and de Rooij, J. (2010). Vinculin potentiates E-cadherin mechanosensing and is recruited to actin-anchored sites within adherens junctions in a myosin II-dependent manner. J. Cell Biol. *189*, 1107–1115.
18. Sebbagh, M., Hamelin, J., Bertoglio, J., Solary, E., and Bréard, J. (2005). Direct cleavage of ROCK II by granzyme B induces target cell membrane blebbing in a caspase-independent manner. J. Exp. Med. *201*, 465–471.
19. Sebbagh, M., Renvoizé, C., Hamelin, J., Riché, N., Bertoglio, J., and Bréard, J. (2001). Caspase-3-mediated cleavage of ROCK I induces MLC phosphorylation and apoptotic membrane blebbing. Nat. Cell Biol. *3*, 346–352.
20. Coleman, M.L., Sahai, E.A., Yeo, M., Bosch, M., Dewar, A., and Olson, M.F. (2001). Membrane blebbing during apoptosis results from caspase-mediated activation of ROCK I. Nat. Cell Biol. *3*, 339–345.
21. Majno, G., and Joris, I. (1995). Apoptosis, oncosis, and necrosis. An overview of cell death. Am. J. Pathol. *146*, 3–15.
22. Barros, L.F., Kanaseki, T., Sabirov, R., Morishima, S., Castro, J., Bittner, C.X., Maeno, E., Ando-Akatsuka, Y., and Okada, Y. (2003). Apoptotic and necrotic blebs in epithelial cells display similar neck diameters but different kinase dependency. Cell Death Differ. *10*, 687–697.
23. Krysko, D.V., Vanden Berghe, T., D'Herde, K., and Vandenabeele, P. (2008). Apoptosis and necrosis: detection, discrimination and phagocytosis. Methods *44*, 205–221.
24. Adams, C.L., Chen, Y.T., Smith, S.J., and Nelson, W.J. (1998). Mechanisms of epithelial cell-cell adhesion and cell compaction revealed by high-resolution tracking of E-cadherin-green fluorescent protein. J. Cell Biol. *142*, 1105–1119.
25. Gumbiner, B.M. (2005). Regulation of cadherin-mediated adhesion in morphogenesis. Nat. Rev. Mol. Cell Biol. *6*, 622–634.
26. Hogan, C., Dupré-Crochet, S., Norman, M., Kajita, M., Zimmermann, C., Pelling, A.E., Piddini, E., Baena-López, L.A., Vincent, J.P., Itoh, Y., et al. (2009). Characterization of the interface between normal and transformed epithelial cells. Nat. Cell Biol. *11*, 460–467.
27. Paluch, E., and Heisenberg, C.P. (2009). Biology and physics of cell shape changes in development. Current biology: CB *19*, R790–R799.
28. Takeichi, M. (1993). Cadherins in cancer: implications for invasion and metastasis. Curr. Opin. Cell Biol. *5*, 806–811.
29. Gottardi, C.J., Wong, E., and Gumbiner, B.M. (2001). E-cadherin suppresses cellular transformation by inhibiting beta-catenin signaling in an adhesion-independent manner. J. Cell Biol. *153*, 1049–1060.
30. Guan, Y., Watson, A.J., Marchiando, A.M., Bradford, E., Shen, L., Turner, J.R., and Montrose, M.H. (2011). Redistribution of the tight junction protein ZO-1 during physiological shedding of mouse intestinal epithelial cells. Am. J. Physiol. Cell Physiol. *300*, C1404–C1414.
31. Balda, M.S., Whitney, J.A., Flores, C., González, S., Cereijido, M., and Matter, K. (1996). Functional dissociation of paracellular permeability and transepithelial electrical resistance and disruption of the apical-basolateral intramembrane diffusion barrier by expression of a mutant tight junction membrane protein. J. Cell Biol. *134*, 1031–1049.
32. Capaldo, C.T., and Macara, I.G. (2007). Depletion of E-cadherin disrupts establishment but not maintenance of cell junctions in Madin-Darby canine kidney epithelial cells. Mol. Biol. Cell *18*, 189–200.
33. Huveneers, S., Oldenburg, J., Spanjaard, E., van der Krogt, G., Grigoriev, I., Akhmanova, A., Rehmann, H., and de Rooij, J. (2012). Vinculin associates with endothelial VE-cadherin junctions to control force-dependent remodeling. J. Cell Biol. *196*, 641–652.

34. Vogel, V., and Sheetz, M. (2006). Local force and geometry sensing regulate cell functions. Nat. Rev. Mol. Cell Biol. *7*, 265–275.
35. Huang, S., and Ingber, D.E. (2000). Shape-dependent control of cell growth, differentiation, and apoptosis: switching between attractors in cell regulatory networks. Exp. Cell Res. *261*, 91–103.
36. Gu, Y., Forostyan, T., Sabbadini, R., and Rosenblatt, J. (2011). Epithelial cell extrusion requires the sphingosine-1-phosphate receptor 2 pathway. J. Cell Biol. *193*, 667–676.
37. Martin, A.C., Gelbart, M., Fernandez-Gonzalez, R., Kaschube, M., and Wieschaus, E.F. (2010). Integration of contractile forces during tissue invagination. J. Cell Biol. *188*, 735–749.
38. Madara, J.L. (1998). Regulation of the movement of solutes across tight junctions. Annu. Rev. Physiol. *60*, 143–159.
39. Koch, S., and Nusrat, A. (2012). The life and death of epithelia during inflammation: lessons learned from the gut. Annu. Rev. Pathol. *7*, 35–60.
40. Vos, C.B., Cleton-Jansen, A.M., Berx, G., de Leeuw, W.J., ter Haar, N.T., van Roy, F., Cornelisse, C.J., Peterse, J.L., and van de Vijver, M.J. (1997). E-cadherin inactivation in lobular carcinoma in situ of the breast: an early event in tumorigenesis. Br. J. Cancer *76*, 1131–1133.
41. Guilford, P., Hopkins, J., Harraway, J., McLeod, M., McLeod, N., Harawira, P., Taite, H., Scoular, R., Miller, A., and Reeve, A.E. (1998). E-cadherin germline mutations in familial gastric cancer. Nature *392*, 402–405.
42. Graziano, F., Humar, B., and Guilford, P. (2003). The role of the E-cadherin gene (CDH1) in diffuse gastric cancer susceptibility: from the laboratory to clinical practice. Ann. Oncol. *14*, 1705–1713.